Multiparametric Labeling Optimization and Synthesis of ^{68}Ga-Labeled Compounds Applying a Continuous-Flow Microfluidic Methodology

Gábor Máté[1], Dezső Szikra[1], Jakub Šimeček[2], Szandra Szilágyi[1], György Trencsényi[1†], Hans-Jürgen Wester[2], István Kertész[1*†] and László Galuska[1]

[1]*Department of Nuclear Medicine, Faculty of Medicine, University of Debrecen, Nagyerdei krt. 98 H-4032 Debrecen, Hungary*
[2]*Lehrstuhl für Pharmazeutische Radiochemie, Technische Universität München, Walther-Meissner Strasse 3, D-85748 Garching, Germany*

Received: 22 January 2016; accepted: 21 March 2016

The synthesis and functional evaluation of a wide variety of radiolabeled chelator–biomolecule conjugates with high specific activity and radiochemical purity are crucial to development of personalized nuclear medicine. An excellent platform technology for achieving this objective involves use of generator-produced positron emission tomography (PET)-radionuclide ^{68}Ga. Currently, applied manual methodology for optimization and development for new labeling techniques offers only slow screening with relatively high precursor consumption. A capillary-based microfluidic synthesis module with online high-performance liquid chromatography (HPLC) was constructed for the optimization of reaction parameters of ^{68}Ga-PET tracers. This approach enables performance of ^{68}Ga-labeling reactions in 10 μL volumes, followed by sample analysis. The high-throughput capacity of the system allows very rapid optimization. The optimal pH and ligand concentration from the experiments were utilized directly to the production of ^{68}Ga-NODAGA-$(RGD)_2$ and ^{68}Ga-NOPO-RGD. Applying optimal parameters to production of these aforementioned radiopharmaceuticals allowed their synthesis with high radiochemical purity (over 95%) and with surprisingly negligible retention of residual activity in the system.

Keywords: ^{68}Gallium, chelators, positron emission tomography, microfluidics, RGD conjugates

1. Introduction

The range of methodologies available to chemists for synthesis of positron emission tomography (PET) tracers has expanded greatly during the last decades. General performance-related expectations from these reactions are that they should be quick, robust, and reproducible. Taking into account these performance requirements along with radiation protection-related factors, remotely controlled automatic or semi-automatic systems have been developed for a diverse number of radiolabeling purposes. For these systems, milligram quantities of precursors are dissolved in several milliliters of a selected solvent to facilitate convenient handling and efficient mixing [1]. Batch-based conventional systems used for the labeling reactions have overcome several practical challenges such as regulatory compliance of operation with Good Manufacturing Practice (GMP) guidelines [2, 3]; they allow high incorporation yields and relatively short reaction times suitable for work with the typically short half-life of the radionuclides.

Presently, the most widely used conventional methods for labeling with PET radionuclides suffer from several significant limitations. The radiation emitted by PET isotopes requires that the devices be located in large, lead-shielded hot cells to protect the staff from the radiation exposure. The concentration of the short-lived PET radionuclides used in the reactions is in the picomolar range [4] and is therefore several orders of magnitude lower than the precursor concentration.

Microfluidic technology emerged in the beginning of the 1980s, and it was developed with the objective of increasing reaction control, conversion yields, and product selectivity, while reducing reaction time and material consumption [5–13]. Currently there are two major trends in the evolution of microfluidics, defined as continuous- and stop-flow setups [14, 15]. The use of microreactors may be used to resolve some of currently existing limitations to biomolecule radiolabeling protocols [1, 16–18]. These constrains include features such as the ability to manipulate small volumes, ensure effective mixing and heat transfer, and the reduction of the system footprint. Numerous microfluidic devices have been described, including commercially available capillary-based microfluidic synthesis platforms [19–21] and lab-on-chip devices [22]. During the early development of this technology, experimental work focused primarily on the synthesis of agents labeled as ^{18}F and ^{11}C. Later, it was recognized that this technique might also be beneficial for radiolabeling with radiometals [23, 24].

Generator-based systems [25] are convenient alternatives to cyclotron produced ^{11}C and ^{18}F [26–28]. Additionally, ^{68}Ga conjugation to small, biocompatible molecules — especially peptides — is a well-established and rapidly growing field, with numerous applications to modern radiopharmaceutical chemistry [29]. Peptide-based receptor ligands possess high affinity and specificity to many varieties of tumor-associated biomolecules. Additionally, in comparison with other biomolecules such as antibodies, peptides are easy to synthesize and characterize, and are rapidly cleared from the blood and nontarget tissues by normal physiological processes [30, 31].

Due to the promising results achieved on the field of PET radiochemistry with microfluid systems and because only a few number of efforts exist to apply this concept with radiometals, we have aimed to develop a new, versatile instrument suitable for speeding up the optimization process, but keeping the potential to scale up the production on the same equipment only with minor modifications. We decided to omit the labor-intensive quality control (QC) method and replace it with a newly developed automatic HPLC protocol, and to testify that the construction can be useful not only for optimization experiments, but for production of radiolabeled peptides for preclinical purpose as well.

Here, we report the development of a new microfluidic device with online analytical/preparative HPLC option. Chemical structures of the investigated compounds that were involved in this study can be seen in Figure 1. A systematic study for direct comparison of the efficiency of manual- and microfluidic labeling of the well-known chelators was

* Author for correspondence: kertesz.istvan@med.unideb.hu
†The authors contributed equally to this study.

DOI: 10.1556/1846.2016.00004

First published online: 3 May 2016

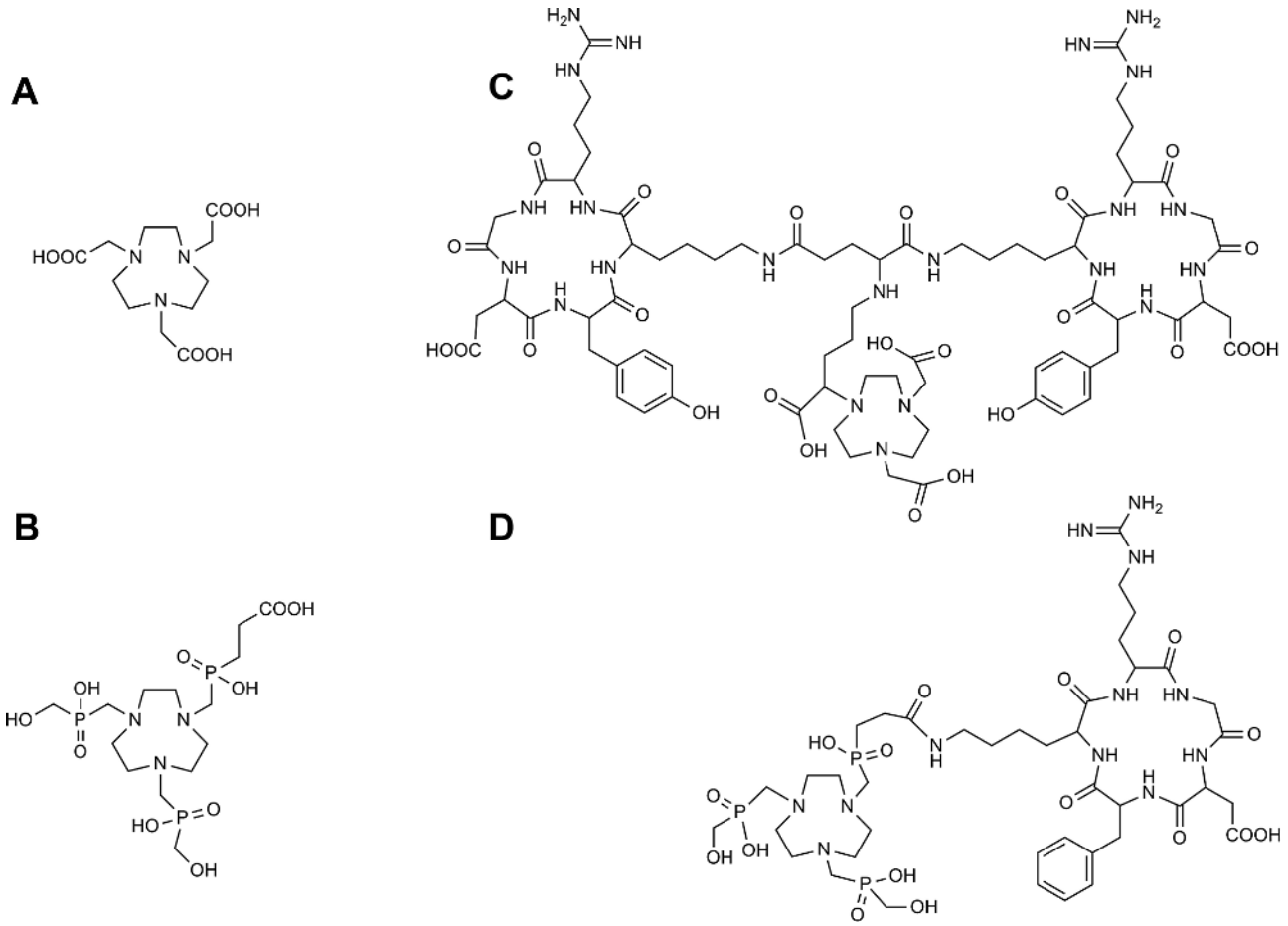

Figure 1. Investigated chemical structures: NOTA (A), NOPO (B), NODAGA-c(RGDyK)$_2$ (C), and NOPO-c(RGDfK) (D)

performed at pH=3. To determine the optimal ^{68}Ga-labeling parameters for NOTA (1,4,7-triazacyclononane-*N*,*N*′,*N*″-triacetic acid) and NOPO [32] (1,4,7-triazacyclononane-1,4-bis [methylene(hydroxymethyl)phosphinic acid]-7-[methylene(2-carboxy-ethyl)phosphinic acid), multiparametric optimization experiments were executed also for verifying the differences experienced in their efficacy performing manual labeling method [32]. The retention of the radiometal in the system was evaluated without complexing agent and in the presence of RGD conjugates of the chelators. This system shows very low ^{68}Ga retention, and it can be a useful tool for high-throughput optimization work of radiometal-labeled biologically active peptides.

2. Results

2.1. Microfluidic System Design. The scheme of the microfluid system can be seen in Figure 2. Base flow in the system was maintained with two KONTRON HPLC pumps (No. 1), which pumped purified water as a carrier fluid. ^{68}Ga solution was introduced from the vials No. 2, while reagents were

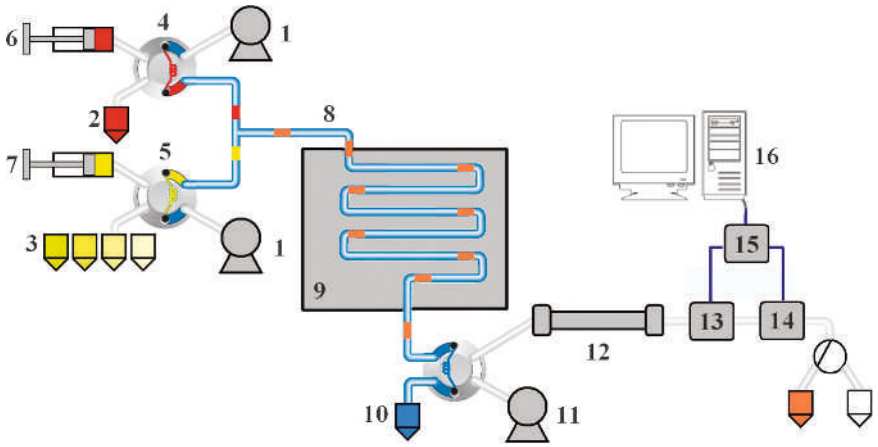

Figure 2. Schematic of the capillary-based microfluidic system for ^{68}Ga-labeling reactions. 1: KONTRON HPLC pumps, 2: vial for ^{68}Ga solution, 3: autosampler vials for reagent solutions, 4 and 5: loop injectors, 6 and 7: syringes in double syringe pump, 8: PEEK reactor (17.5 m×0.15 mm), 9: air thermostat, 10: waste, 11: HPLC pump (Waters LC module integrated HPLC system), 12: HPLC column, 13: ATOMKI radioactivity detector, 14: UV detector (Waters LC module integrated HPLC system), 15: data acquisition module, and 16: PC

injected from the autosampler vials No. 3. Every synthesis cycle was initialized by loading the reagents into the loops (at loop injector Nos. 4 and 5) by means of the double syringe pump equipped with syringes Nos. 6 and 7. Automated radiolabeling reactions were started with the coinjection of the solutions into the PEEK reactor (No. 8). The mixture of the chelator and radiometal solutions is carried through the PEEK capillary that is reeled in an air thermostat (No. 9). The reaction mixture can be collected through an outlet (No. 10) or – depending on the automated protocol – a sample of it can be injected on an online HPLC system (Nos. 11–15) for instant analysis.

The system was controlled by an Arduino Mega 2560R3 microcontroller card. The code was written in Arduino language.

2.2. Method Validation. Radiolabeling optimization experiments were performed using NOTA and NOPO chelators with the newly developed microfluidic system and with the conventional, manual labeling methodology, under identical parameters: 5-min reaction time, 95 °C, and pH 3.0. The radiochemical purity % (RCP) of the resulting mixtures was determined by cation-exchange-based online HPLC after microfluidic labeling, while thin-layer chromatography (TLC) analysis was performed in the case of manual labeling. Comparative results can be seen in Figure 3.

The radiochemical purity–concentration curves are very similar, independently from the selected techniques. When comparing the labeling curves of NOTA, it can be observed that both the microfluidic and the manual labeling appoints the very same concentration region for reaching quantitative labeling results (>95%), and this region starts with ligand concentration 1 μM, as the edge of the curve. Moreover, almost no difference can be found in the intermediary zone of 0.1–0.3 μM.

Interestingly, the results are not exactly the same for NOPO. Despite that the ligand concentration–radiochemical purity curves show a similar shape and they both appoint the concentration region starting from 0.1 μM as a suitable zone for performing quantitative labeling, here, microfluidic labeling performed better and, still, quantitative labeling was found under the investigated reaction conditions for labeling with NOPO at 0.03 μM concentrations.

2.3. Multiparametric Labeling Optimization. Similarly to the method validation – as test molecules – NOTA and NOPO were evaluated with the automated methodology. In order to find optimal microfluidic labeling parameters, both chelators were analyzed for ^{68}Ga-labeling in the ligand concentration range from 100 to 0.01 μM and in the pH range from 1 to 9 with the constant reaction parameters (5-min reaction time and 95 °C reaction temperature). The measurement results were collected in a few hours for each substance, and the only necessary human assistance was the regular change of the decayed, HEPES-buffered (4-(2-hydroxyethyl)piperazine-1-ethanesulfonic acid) ^{68}Ga solution after every 9 measurements.

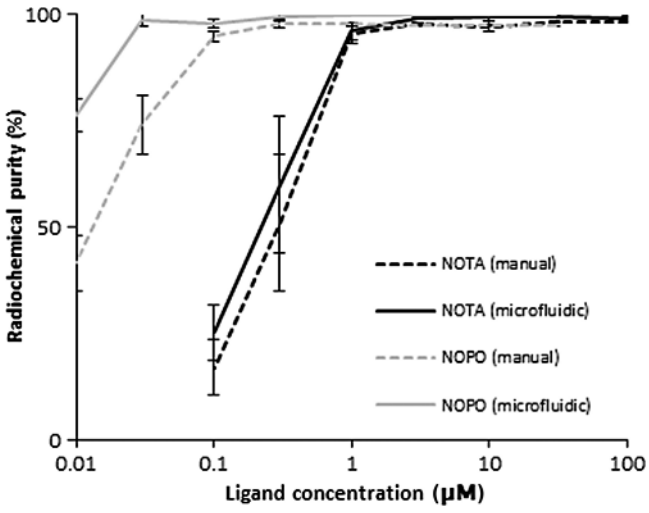

Figure 3. Comparison of radiochemical purity (%) of ^{68}Ga-NOTA and ^{68}Ga-NOPO produced with manual and microfluidic labeling protocols (reaction parameters: concentration of HEPES = 1.75 M, 5 min, 95 °C, and pH 3.0 (n = 3))

In accordance with general expectations towards radiopharmaceutical products, RCP > 95%, results were evaluated as appropriate for further synthetic use. As it can be seen in Figure 4A and B, measured values were represented on a 3D graph, where the quantitative value can be found for each investigated parameter. Moreover, for simple, qualitative evaluation of the labeling experiments, the very same results were depicted on a 2D graph as well.

For NOTA (Figure 4A and C), appropriately high RCP values (red zone) were found in the 3–7 pH region. The highest efficiency in complex formation and, thus, the lowest ligand concentration suitable for quantitative labeling were found at pH 3.0–4.0 and 3 μM NOTA.

On the other hand, for NOPO, our results show a different pattern (Figure 4B and D). Here, quantitative labeling can be granted among broader combination of labeling conditions. High radiochemical purity can be accomplished on the pH scale 1–7, which means a significant extension compared to NOTA which bears an identical triazacyclononane ring but differently substituted pendant arms. Moreover, the zone of efficient labeling extended toward the lower concentrations also and reached the 0.03–0.3 μM values at pH 3.0.

Nevertheless, robustness in terms of pH and ligand concentration had to be taken into consideration as in a continuous-flow system reaction mixture is expected to be diluted with the carrier fluid because of the laminar flow. As such, for appropriate robustness, pH 3.0 and 10 μM concentration for NOTA and 1 μM concentration for NOPO were chosen as "optimal" reaction parameters for further synthetic evaluation of the investigated system.

2.4. ^{68}Ga Retention in the PEEK Capillary System. Retention of the radionuclide in the PEEK capillary system that serves as a nonconventional reaction vessel when performing our microfluidic labeling reactions was measured in the pH range of 1–9. At every case, the system was heated to 95 °C, and 5-min residence time was adjusted by application of the flow rate to 0.066 mL/min. The measured retention values can be seen in Figure 5.

By our results, no retention can be found in the system at pH values 8 and 9. However, decrementing the pH values from 7 to 3, the ratio of the retained radioactivity increases gradually. This process reaches its maximum at pH 3, where more than 90% of the injected activity is missing from the collected effluent. Surprisingly, after additional decrease of the pH value of the flowing mixture, this retention completely vanishes, and no retention of the nuclide was observed at the highly acidic pH values of 1 and 2.

2.5. Microfluidic Syntheses with ^{68}Ga. In order to test the utility of the microfluidic system, direct microfluidic syntheses with NOTA and NOPO [32, 33], and their respective RGD conjugates, NODAGA-c(RGD)$_2$ and NOPO-RGD [34, 35], were performed. Synthetic parameters were chosen based upon the results of the multiparametric labeling optimization studies for NOTA (c_{ligand} = 10 μM; pH 3.0) and NOPO (c_{ligand} = 1 μM; pH 3.0), and – for the verification of the collected data – identical parameters were applied for the microfluidic labeling of their corresponding conjugates. All reactions were performed

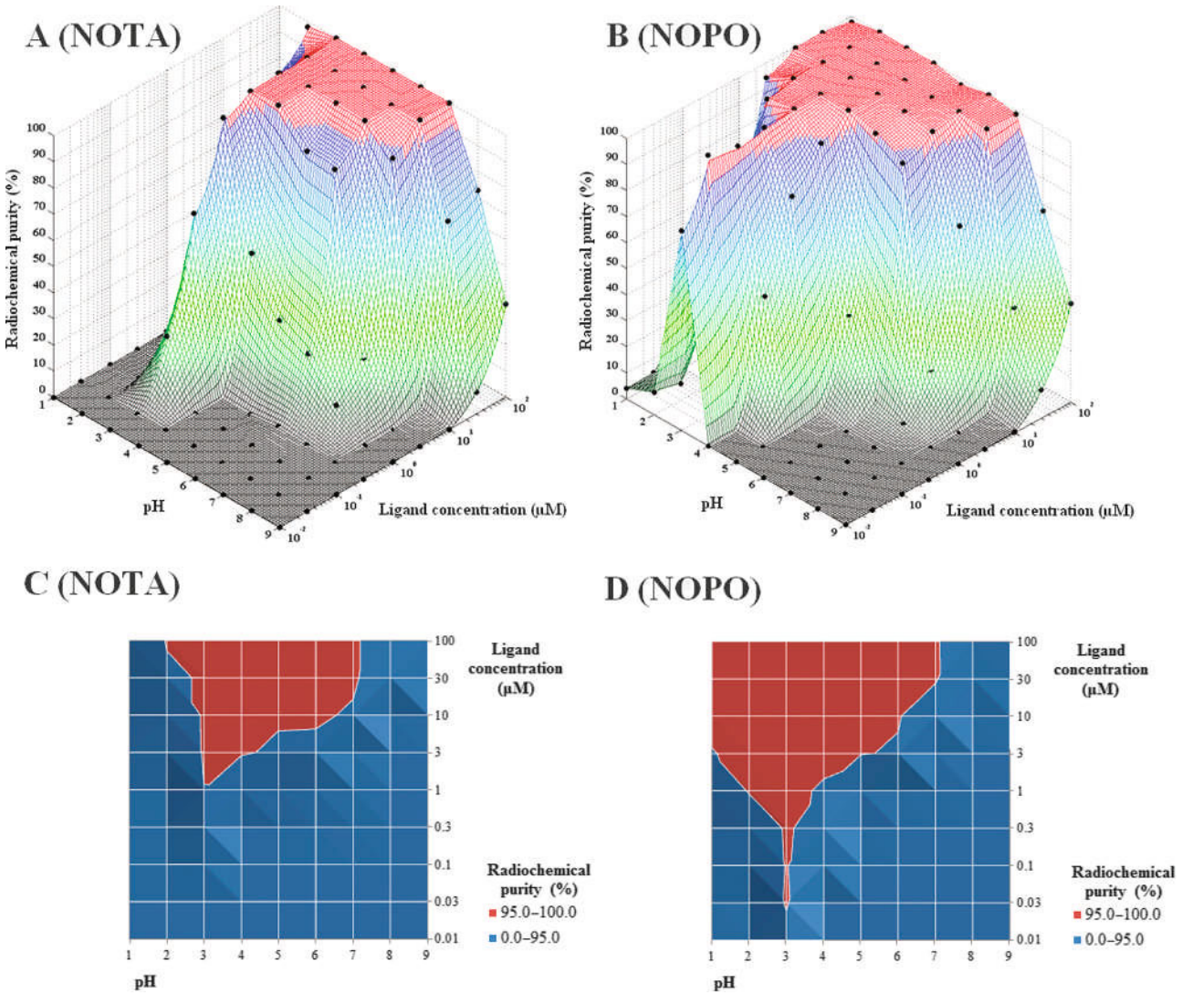

Figure 4. Sequential analysis of labeling properties of the investigated chelators with differing ligand concentration values and at different pH with the fixed parameters of 5-min reaction time and 95 °C. Results are depicted on a 3D-graph with a generated surface (black dots represent measured values) for NOTA (A) and NOPO (B). For the evaluation of the quantitative labeling region (RCP (radiochemical purity) > 95%), the very same results are depicted on a 2D-graph (measured values at grids) for NOTA (C) and NOPO (D). Red zones represent > 95% RCP values for the corresponding labeled compound everywhere

at 95 °C. The coinjected 10–10 μL reactant solutions were collected in a 30–50 μL final volume depending on the applied flow rate.

The "recovered" activity was more than 95% at every run; no significant retention was found for the labeled compounds in the PEEK capillary system. Additionally, the overall radiochemical purities of the mixtures were excellent; quantitative complex formation (RCP%≥95%) was measured everywhere (Table 1).

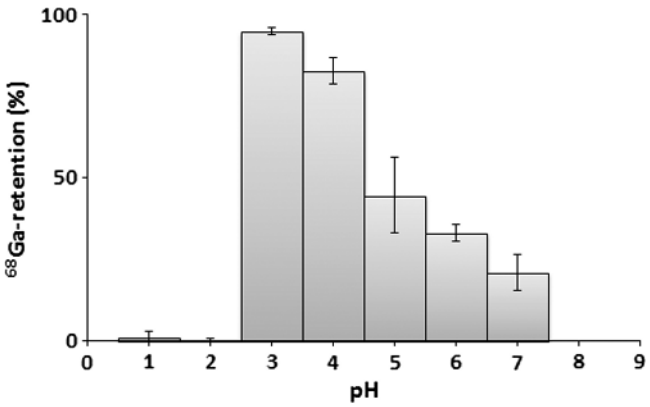

Figure 5. Measured retention (%) of ^{68}Ga in the PEEK capillary system at different pH values. Measurement parameters: concentration of HEPES = 1.75 M, 5-min residence time, and 95 °C (n = 3)

After experiencing excellent synthetic results with the chelators at 5 min, we increased the flow rate in the system from 0.066 mL/min to 0.132 and 0.264 mL/min and, thus, decreased reaction (residency) time from the original 5 min to 2.5 and 1.25 min for NOTA and NOPO. Our measurements show that no significant reduction of the radiochemical purity can be observed, which suggests that the rate of the complex formation with the radiometal for these chelators is much higher than it could be expected.

3. Discussion

Microfluidic labeling offers an alternative route for the synthesis of several well-known ^{18}F- and ^{11}C-labeled radiopharmaceuticals. Nevertheless, in the case of PET radiometals, the numbers of studies are few and the ability to predict outcomes based on experimental design is significantly constrained. Batch-based PDMS-chip reactor synthesis of ^{64}Cu-DOTA-c(RGDfK) was performed by Wheeler et al. [23]. Additionally, a similar PDMS chip-based synthetic methodology was considered for production of DOTA-c(RGDfK), NOTA-c(RGDfK),

Table 1. Microfluidic synthesis results for radiolabeling with ^{68}Ga of NOTA, NOPO, NODAGA-c(RGD)$_2$, and NOPO-RGD at 95 °C and pH 3.0 (n = 3)

Ligand	Ligand concentration (μM)	Flow rate (mL/min)	Reaction time (min)	^{68}Ga recovery (%)	Radiochemical purity (%)
NOTA	10	0.066	5	99	99
		0.132	2.5	98	99
		0.264	1.25	98	99
NOPO	1	0.066	5	100	98
		0.132	2.5	97	98
		0.264	1.25	100	99
NODAGA-c(RGD)$_2$	10	0.066	5	96	99
NOPO-RGD	1	0.066	5	99	97

and DOTA-BSA, labeled with ^{64}Cu and ^{68}Ga by Zeng et al. [24]. In each of the aforementioned, successful syntheses were described for the previously described PET-diagnostic agents. Also for these cases, higher reaction yields were achieved using microfluidic labeling versus conventional synthesis. The authors of this report utilized nonradioactive metals for adjusting the exact concentration of metal ions and, thus, regulating chelator/metal ratio. Quantitative labeling was reported as a correlate of chelator–metal ratios utilized. Additionally, experiments with no-carrier added radiometals were also performed. Outcomes of these experiments demonstrated that quantitative labeling could be accomplished only in case of a reasonable excess of the chelators which obviously decreases specific activity of the final product.

In contrast to previous studies, the present investigation describes a microfluidic methodology, in which a PEEK capillary is used as a nonconventional reactor for the noncarrier added synthesis of ^{68}Ga-labeled radiopharmaceuticals. The tube is reeled up inside an air thermostat for accurate temperature control. NOTA and NOPO are well-known for their ^{68}Ga chelation properties [32, 33]; thus, they were chosen as model compounds for testing the operation of the new system. Moreover, new HPLC method was developed for the separation of labeled chelators and "free" ^{68}Ga. By comparing the results of the manual labeling and microfluidic procedure, we established correlation for the two applied methods which allowed for validation of the microfluidic approach. The methods provided slightly different results only in extremely low concentrations of NOPO. Such a deviation was considered typical for the threshold limits.

Further evaluation of the continuous-flow microfluidic system was focused on the utilization of the high-throughput and minimal human interaction properties of this setup. Here, we performed sequential analysis of labeling properties of the chelators NOTA and NOPO under microfluidic conditions over a broad range of reaction parameters: 0.01–100 μM ligand concentration and 1–9 pH range. The temperature and the reaction time were maintained stably at 95 °C for 5 min (Figure 4). Similarly to previous reports [36, 37], NOPO with its phosphinic pendant arms exhibited an extended labeling profile in comparison with NOTA. This was observed at the lowest ligand concentration needed for achieving quantitative labeling. Additionally, radiochemical purity over 95% was obtained on a broader pH scale. NOPO preserves its affinity towards ^{68}Ga in highly acidic pH values of 1 and 2 as well.

A PEEK capillary apparatus was chosen as a nonconventional reactor, since this device has been successfully utilized as a component of multiple-use radiochemical systems due to its compatibility with basic, acidic, and organic solvent and high temperature (up to 134 °C) conditions [38]. Additionally, being an organic polymer, no significant reactivity was expected with the reagents used for ^{68}Ga-labeling reactions. In our system, ^{68}Ga retention was measured at carefully defined pH values, since aqueous Ga(III) can be present in many forms. In these studies, an interesting retention pattern was observed: significant ^{68}Ga retention was measured between pH values of 3–7 with the maximum at pH 3 (Figure 5). Depending on the composition of the solution, aqueous gallium is known to form different hydroxo-complexes [Ga(OH)$_n$] in this pH region [39], but it is also known to be more dominant with the increase of the pH value of the solution. This process appears to be the reverse of the measured tendency. Therefore, we hypothesized that the trend towards retention may be a consequence of the buffer system. HEPES is supposed to form a weak complex with aqueous Ga(III) [40] and has a pK_a value at 2.99 [41]. ^{68}Ga, as a component of an organic complex, might possess a higher affinity for adsorption than aqueous Ga(III) alone. Alteration in the charge at pH 3 can affect the existence of the proposed weak complex and, therefore, the activity retention itself. The possible involvement of the buffering reagents used in the system in terms of the activity retention was also described by Szikra et al. [42]. Moreover, pH 3 appears to be an optimally productive condition for that described in the present report. This finding also suggests a change in the transchelation process which occurs at pH 3.

Test syntheses were also performed to determine the suitability of PEEK reactor for preparative purpose also. In these experiments, activity retention was measured in the presence of different chelators/chelator–peptide conjugates. Parameters of the system optimal for synthesis of desired conjugates were chosen with the objective of achieving required robustness since, in a continuous-flow system, dilution with the carrier fluid can be expected. In these experiments, concentrations of 10 μM for NOTA and 1 μM for NOPO were selected, both at pH 3.0. These concentration values are at least one measurement step higher than the lowest ligand concentration needed for quantitative labeling. Moreover, when productivity of the system was tested at higher pH values, RCP over 95 % was still obtained (Figure 4). In these test runs, identical reaction parameters were also used for the analogous peptide conjugates of the chelators as well.

NOTA, NOPO, and their respective analogues conjugated with RGD peptides; NODAGA-c(RGD)$_2$ and NOPO-RGD were studied, and the analysis of final reaction mixtures demonstrated that only marginal or negligible retention (<5%) may be expected in the presence of the chelating moieties investigated in the present study.

4. Conclusion

Here, a ^{68}Ga-labeling approach was evaluated using an in-house built microfluidic system equipped with online HPLC. This methodology allows efficient evaluation of optimal reaction parameters (temperature, reaction time, pH, ligand concentration) in an automated manner with minuscule precursor consumption. We could demonstrate that complete parametric evaluation of the labeling conditions for a chelator could have been completed within one working day, without requirement for permanent presence of an operator, using the microfluidic methodology. By contrast, the manual approach typically requires 2 to 3 days of intensive work per chelator/conjugate. Moreover, we have demonstrated that, in presence of a chelator/chelating moiety, ^{68}Ga-labeling reactions may be performed

with excellent radiochemical purity (>95%) and with no significant retention (<5%) in the capillary system.

The microfluidic approach might serve as a high-throughput standardized tool for evaluation of novel chelators for ^{68}Gallium and other PET radiometals. Scale-up synthesis for production of clinical doses of ^{68}Ga-PET radiopharmaceuticals has been evaluated separately.

5. Experimental

5.1. General. All commercially available chemicals were of analytical grade and used without further purification. For the radiolabeling studies, Ultrapur® water, HCl, and NaOH were obtained from Merck. NOTA was the product of Chematech (Dijon, France), and NODAGA-c(RGD)$_2$ was purchased from ABX GmbH. All other chemicals were the product of Sigma-Aldrich, if not specifically stated otherwise.

NOPO and NOPO-RGD were synthesized and characterized as published by Šimeček et al. [36]. Independently of the exact chemical form of ^{68}Ga(III) in the aqueous solution, not chelated ^{68}Ga(III) was considered as "free" ^{68}Ga everywhere.

5.2. Manual Labeling. Manual labeling was performed according to the procedure described by Notni et al. [37]. Briefly, ^{68}Ga was eluted from a SnO_2-based ^{68}Ge/^{68}Ga-generator (iTHEMBA Labs, Cape Town, South Africa with 1 M HCl (aq.). A fraction of 1250 μL volume containing the highest activity (≈200 MBq) was collected and buffered with HEPES (800 μL, aq., 5 M). Ninety-microliter aliquots of that solution were added to 10 μL of ligand stock solutions (pH≈3.0) and kept for 5 min at 95 °C. After a quick cooling of the reaction mixtures, samples were taken and ^{68}Ga incorporation (%) was determined by instant thin-layer chromatography (ITLC) on silica-impregnated chromatography paper (Varian Inc.) (mobile phase: 1 M aq. NH_4OAc–MeOH, 1:1). Scanning and evaluation were performed with a MiniGITA Star TLC-scanner (Raytest). In all cases, labeling was considered to be quantitative when at least 95% radiochemical purity was found for the labeled compound based on the resulting chromatogram.

5.3. Operation of the Microfluidic Synthesis Module Combined with Online HPLC System. Timetable of automated operation of the microfluidic system for sequential evaluation of chelating moiety bearing substances can be seen in Figure 6 (down) (for the composition of the system, see Figure 2). The whole process starts with the coinjection of 10–10 μL of the reagent solutions from loop injectors to the continuous flow of water (water for injection) in the PEEK capillary system. Flow is set to 0.066 mL/min for 5-min residence time in the air tempered section of the reactor tube. The thermostat was adjusted to 95 °C at all our measurements. Due to the high surface area and excellent thermal conduction, the effluent liquid was measured to reach room temperature just after dropping out from the capillary. The output of the reactor was attached to a third HPLC injector valve, equipped with a 20-μL loop, which automatically injected the reaction mixture to the HPLC column. Separation of the radioactive components was performed on an Adsorbosphere® XL SCX column with a gradient of NaCl solution. Data acquisition was started with the coinjection of the reagent solutions; as such, the retention times on the resulting chromatograms were 9.7 min for ^{68}Ga-NOPO, 12.0 min for ^{68}Ga-NOTA, and 15.3 min for "free" ^{68}Ga (net retention times in the HPLC system for ^{68}Ga-NOPO, ^{68}Ga-NOTA, and "free" ^{68}Ga were 4.7, 7.0, and 10.3 min, respectively.).

Equilibration of the column to initial conditions between two injections was done at the same time as the next reaction mixture was flowing in the reactor tube. A typical HPLC chromatogram of the SCX-based online analysis can be seen in Figure 6 (up).

5.4. Microfluidic Labeling and Online Analysis. Fraction of 1250 μL from the highest activity concentration eluate (≈200 MBq) was collected and buffered with HEPES solution (see manual labeling). This solution was placed into the microfluidic module (Figure 2 (2)). As the module is suitable for the mixing of reaction solutions in 1:1 ratio, aqueous chelator solutions were prepared by addition of HEPES and the pH was adjusted by HCl or NaOH. In these experiments, the final HEPES concentration in the reaction mixture was≈1.75 M. The chelators were investigated in the 100–0.01 μM (100, 30, 10, 3, 1, 0.3, 0.1, 0.03, 0.01 μM) concentration and in the 1–9 pH range. The buffered chelator solutions were placed into the autosampler (Figure 2 (3)). When the microfluidic labeling optimization studies were performed, analytical evaluation of the reaction mixtures was done automatically by instant injection of a 20-μL sample to the online HPLC system. RCP of NOTA and NOPO was evaluated using Adsorbosphere® XL SCX column (250×4.6 mm) with 5 μm silica (90 Å pore size). A linear gradient elution (see Table 2, to the left) with water (eluent A), 0.2 M tartaric acid aq. solution, pH=2 (eluent B), and 5% NaCl aq. solution (eluent C) was used at a flow rate of

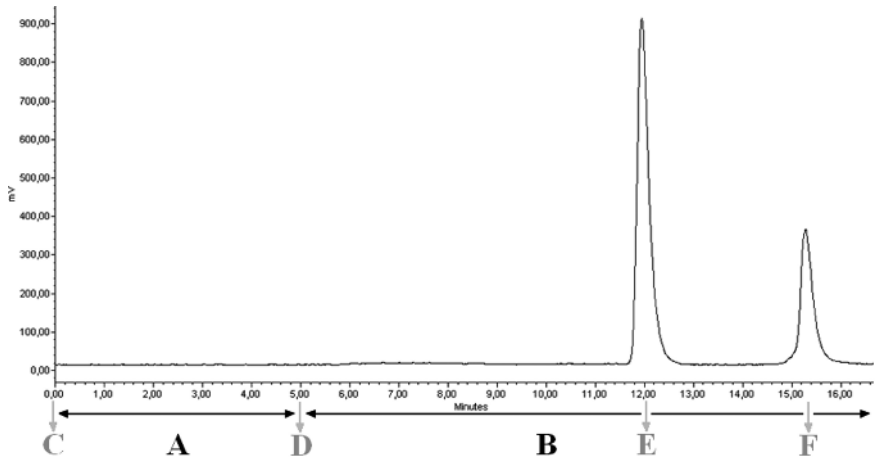

Figure 6. Typical HPLC chromatogram from a sequential analysis of ^{68}Ga-labeling properties of NOTA (up), underlying processes of combined microfluidic HPLC system on the very same time scale (down). Sequential analysis consisted of two main processes: reaction mixture flowing the PEEK reactor system — while washout period from previous injection for the HPLC column (A), HPLC separation of the radioactive compounds of the final mixture (B) with the following important related events: initial coinjection of the reagent solutions (C), sample injection of the final reacted mixture to HPLC system — while instant start of NaCl-solution gradient (D), detection of ^{68}Ga-NOTA (E) and "free" ^{68}Ga (F)

Table 2. Gradient elution used with Adsorbosphere® SCX for the analysis of reaction mixtures with NOTA and NOPO (to the left) and gradient elution used with Kinetex XB C18 for the analysis of reaction mixtures with NODAGA-c(RGD)$_2$ and NOPO-RGD (to the right)

Separation method for the investigated chelators		Separation method for the investigated chelator conjugates	
Eluents used: water (A), 0.2 M tartaric acid aq. solution, pH=2 (B), and 5 % NaCl aq. solution (C)		0.1% H_3PO_4 (eluent A) and ACN (eluent B)	
Time point (min)	% of mixing	Time point (min)	% of mixing
0	65% A, 30% B, 5% C	0	100% A
5	65% A, 30% B, 5% C	5	100% A
7	0% A, 30% B, 70% C	7	20% A
13	0% A, 30% B, 70% C	9.5	20% A
		9.6	100% A

1 mL/min. Ultraviolet (UV) detector (Waters Integrated LC Module Plus) was set at 210 nm in combination with RA detector (ATOMKI). RCP% was determined from the AUC values of their peaks on the corresponding RA chromatogram using decay correction. For RGD conjugates, Kinetex XB C18 2.6 μm 50×4.6 mm column was used with a gradient elution (see Table 2, to the right) of 0.1% H_3PO_4 (eluent A) and ACN (eluent B) at a flow rate of 1 mL/min.

5.5. Method Validation. Direct comparison of manual and microfluidic labeling methodology for the testing of the ^{68}Ga-binding properties of different chelator systems was performed. All labeling experiments were done according to the aforementioned protocols with fixed parameters of pH 3.0, 95 °C, and 5-min reaction time. Labeling properties of NOTA and NOPO were compared on a broad concentration scale (100, 30, 10, 3, 1, 0.3, 0.1, 0.03, 0.01 μM) with both methods.

5.6. Multiparametric Labeling Optimization. The investigated compounds were evaluated in the concentration range of 100–0.01 μM (series of concentration values applied: 100, 30, 10, 3, 1, 0.3, 0.1, 0.03, 0.01 μM) and in the pH range of 1–9 (pH values in order 1, 2, 3, …, 9) for 5 min (0.066 mL/min flow rate in a 17.5 m×0.15 mm PEEK capillary) and constant reaction temperature of 95 °C. Radiochemical purity was measured by automated injection of all samples to the online HPLC system, applying the cation-exchange method with Adsorbosphere® XL SCX column.

5.7. ^{68}Ga Retention in the PEEK Capillary System. Retention of the radionuclide in the PEEK capillary system was tested by coinjection of ^{68}Ga- and buffer solutions at various pH values. Stock solution for the "free" radiometal (preparation described in microfluidic labeling) was loaded into the system. It was mixed in the microfluidic system with aqueous "blank" solutions that were prepared identically to the microfluidic labeling studies, but without any chelator. Radionuclide retention in the system was calculated from the decay-corrected value of the measured activity of the effluent solution after coinjection of 10–10 μL of HEPES-buffered ^{68}Ga and "blank" solutions running through the whole system. Injected activity was measured directly from the autosampler without reactor capillary. At these cases, activities of all collected samples were measured after a 90-min decay time with a Canberra Packard Cobra II gamma counter. ^{68}Ga retention in the system was determined separately for all individual pH values.

5.8. Microfluidic Syntheses with ^{68}Ga. In order to evaluate the potential utility of the microfluidic system for large scale synthesis, a combined measurement protocol – involving both retention and radiochemical purity analyses – was performed for all investigated substances. Syntheses were accomplished by coinjection of 10–10 μL of reagents (as described in Section Microfluidic Labeling and Online Analysis). The product solution was collected by dropwise fractionation of the effluent liquid from the system. Radioactivity values of the collected samples were measured instantly with a Canberra GC 1020 gamma spectrometer using the AUC values of the energy peak of 511 keV. Similarly to the previous retention study, ^{68}Ga recovery was calculated as the ratio of collected and injected radioactivity. Afterwards, a sample was taken and it was injected to the HPLC for the determination of radiochemical purity.

Synthetic parameters of ligand concentration and pH were chosen based upon the results of the multiparametric labeling optimization studies for NOTA and NOPO and to evaluate the relevancy of the collected data — the very same parameters were applied for the microfluidic labeling of their conjugates, NODAGA-c(RGD)$_2$ and NOPO-RGD. Reaction temperature remained unchanged at 95 °C. Experiments to reduce the reaction time – from 5 min to 2.5 and 1.25 min – by increasing the flow rate from 0.066 mL/min to 0.132 and 0.264 mL/min was also performed for NOTA and NOPO.

Conflicts of Interest

The authors declare no conflict of interest.

Acknowledgments. The contribution of the first author to this research project was supported by the European Union and the State of Hungary, cofinanced by the European Social Fund in the framework of TÁMOP-4.2.4.A/2-11/1-2012-0001 "National Excellence Program."

References

1. Elizarov, A. M.; van Dam, R. M.; Shin ,Y. S.; Kolb, H. C.; Padgett, H. C.; Stout, D.; Shu, J.; Huang, J.; Daridon, A.; Heath, J. R. *J. Nucl. Med*. **2010**, *51*, 282–287.
2. Boschi, S.; Malizia, C.; Lodi, F. *Recent Results Cancer Res*. **2013**, *194*, 17–31.
3. Boschi, S.; Lodi, F.; Malizia, C.; Cicoria, G.; Marengo M. *Appl. Radiat. Isot*. **2013**, *76*, 38–45
4. Fuchtner, F.; Preusche, S.; Mading, P.; Zessin, J.; Steinbach, *J. Nuklearmedizin. Nucl. Med*. **2008,** *47*, 116–119
5. Lee, C. C.; Sui, G.; Elizarov, A.; Shu, C. J.; Shin, Y. S.; Dooley, A. N.; Huang, J.; Daridon, A.; Wyatt, P.; Stout, D.; Kolb, H. C.; Witte, O. N.; Satyamurthy, N.; Heath, J. R.; Phelps, M. E.; Quake, S. R., Tseng, H. R. *Science* **2005**, *310*, 1793–1796.
6. Roberge, D. M.; Ducry, L.; Bieler, N.; Cretton, P.; Zimmerman, B. *Chem. Eng. Technol*. **2005**, *28*, 318–323.
7. Lu, S. Y.; Pike, V. W. *The Driving Force in Molecular Imaging*; Schubiger, P. A.; Lehmann, L.; Friebe, M., Eds.; Springer-Verlag: Heidelberg, 2006; pp. 271–289.
8. Watts, P.; Haswell, S. J. *Chem. Eng. Technol*. **2005**, *28*, 290–301.
9. Kang, L.; Chung, B. G.; Langer, R.; Khademhosseini, A. *Drug Discov. Today* **2008**, *13*, 1–13.
10. Huebner, A.; Sharma, S.; Srisa-Art, M.; Hollfelder, F.; Edel, J. B.; de Mello, A. J. *Lab Chip* **2008**, *8*, 1244–1254.
11. Miller, P. W. *J. Chem. Technol. Biotechnol*. **2009**, *84*, 309–315.
12. Fortt, R.; Gee, A. *Future Med. Chem*. **2013**, *5*, 241–244.
13. Pascali, G.; Watts, P.; Salvadori, P. A. *Nucl. Med. Biol*. **2013**, *40*, 776–787, 8–323.
14. Elizarov, A. M. *Lab Chip* **2009**, *9*, 1326–1333.
15. Keng, P. Y.; Esterby, M.; van Dam, R. M. In *Positron Emission Tomography — Current Clinical and Research Aspects*; Hsieh, C.-H. Ed.; InTech, DOI: 10.5772/31390. Available from: http://www.intechopen.com/books/positron-emission-tomography-current-clinical-and-research-aspects/emerging-technologies-for-decentralized-production-of-pet-tracers.
16. Gillies, J. M.; Prenant, C.; Chimon, G. N.; Smethurst, G. J.; Dekker, B. A.; Zweit, J. *Appl. Radiat. Isot*. **2006**, *64*, 333–336.
17. Audrain, H. *Angew. Chem., Int. Ed. Engl*. **2007**, *46*, 1772–1775.
18. Lebedev, A.; Miraghaie, R.; Kotta, K.; Ball, C. E.; Zhang, J.; Buchsbaum, M. S.; Kolb, H. C.; Elizarov, A. *Lab Chip* **2013**, *13*, 136–145.
19. Briard, E.; Zoghbi, S. S.; Siméon, F. G.; Imaizumi, M.; Gourley, J. P.; Shetty, H. U.; Lu, S.; Fujita, M.; Innis, R. B.; Pike, V. W. *J. Med. Chem*. **2009**, *52*, 688–699.

20. Wester, H. J.; Schoultz, B. W.; Hultsch, C.; Henriksen, G. *Eur. J. Nucl. Med. Mol. Imaging* **2009**, *36*, 653–658.
21. Pascali, G.; Mazzone, G.; Saccomanni, G.; Manera, C.; Salvadori, P. A. *Nucl. Med. Biol.* **2010**, *37*, 547–555.
22. Liu, K.; Lepin, E. J.; Wang, M. W.; Guo, F.; Lin, W. Y.; Chen, Y. C.; Sirk, S. J.; Olma, S.; Phelps, M. E.; Zhao, X. Z.; Tseng, H. R.; Michael van Dam, R.; Wu, A. M.; Shen, C. K. *Mol. Imaging* **2011**, *10*, 168–176.
23. Wheeler, T. D.; Zeng, D.; Desai, A. V.; Onal, B.; Reichert, D. E.; Kenis, P. J. *Lab Chip* **2010**, *10*, 3387–3396.
24. Zeng, D.; Desai, A. V.; Ranganathan, D.; Wheeler, T. D.; Kenis, P. J.; Reichert, D. E. *Nucl. Med. Biol.* **2013**, *40*, 42–51.
25. Rösch, F. *Appl. Radiat. Isot.* **2013**, *76*, 24–30
26. Decristoforo, C. *Curr. Radiopharm.* **2012**, *5*, 212–220.
27. Lee, V. S. *Recent Results Cancer Res.* **2013**, *194*, 43–75.
28. Velikyan, I. *Theranostics* **2014**, *4*, 47–80.
29. Morgat, C.; Hindié, E.; Mishra, A. K.; Allard, M.; Fernandez, P. *Cancer Biother. Radiopharm.* **2013**, *28*, 85–97.
30. Decristoforo, C.; Pickett, R. D.; Verbruggen, A. *Eur. J. Nucl. Med. Mol. Imaging* **2012**, Suppl. 1, S31–S40.
31. Máté, G.; Kertész, I.; Enyedi, K. N.; Mező, G.; Angyal, J.; Vasas, N.; Kis, A.; Szabó, É.; Emri, M.; Bíró, T.; Galuska, L.; Trencsényi, Gy. *Eur. J. Pharm. Sci.* **2015**, *69*, 61–71.
32. Šimeček, J.; Hermann, P.; Wester, H. J.; Notni, J. *ChemMedChem.* **2013**, *8*, 95–103.
33. Notni, J.; Šimeček, J.; Wester, H. J. *ChemMedChem.* **2014**, *9*, 1107–1115 (corrigendum: ibid. **2014**, *9*, 2614).
34. Šimeček, J.; Zemek, O.; Hermann, P.; Notni, J.; Wester, H. J. *Mol. Pharmaceutics* **2014**, *11*, 3893−3903.
35. Šimeček, J.; Notni, J.; Kapp, T. G.; Kessler, H.; Wester, H. J. *Mol. Pharmaceutics.* **2014**, *11*, 1687–1695.
36. Šimeček, J.; Zemek, O.; Hermann, P.; Wester, H. J.; Notni, J. *ChemMedChem* **2012**, *7*, 1375–1378.
37. Notni, J.; Šimeček, J.; Hermann, P.; Wester, H. J. *Chem. Eur. J.* **2011**, *17*, 14718–14722.
38. Rensch, C.; Jackson, A.; Lindner, S.; Salvamoser, R.; Samper, V.; Riese, S.; Bartenstein, B.; Wängler, C.; Wängler, B. *Molecules* **2013**, *18*, 7930–7956.
39. Baes, C. F.; Mesmer, R. E. *The Hydrolysis of Cations*, John Wiley & Sons: New York, 1976; pp. 320–322.
40. Martins, A. F.; Prata, M. I.; Rodriguese, S. P.; Geraldes, C. F.; Riss, P. J.; Amor-Coarasa, A.; Burchardt, C.; Kroll, C.; Roesch, F. *Contrast Media Mol. Imaging* **2013**, *8*, 265–273.
41. Sokolowska, M.; Bal, W. J. *Inorg. Biochem.* **2005**, *99*, 1653–1660.
42. Szikra, D.; Mate, G.; Nagy, G. J. *Nucl. Med.* **2015**, *56*, 75.